




New tuning formulas for a nonlinear PID control scheme

Yung-Deug Son¹ · Gang-Gyoo Jin² · Tefera T. Yetayew² ·
Pikaso Pal³ 

Received: 7 June 2022 / Revised: 18 July 2023 / Accepted: 8 August 2023 / Published online: 18 August 2023

© The Author(s) under exclusive licence to The Society for Reliability Engineering, Quality and Operations Management (SREQOM), India and The Division of Operation and Maintenance, Lulea University of Technology, Sweden 2023

Abstract Many processes operated in chemical process industries show time-varying and highly nonlinear characteristics. This paper proposes an enhanced nonlinear PID (NPID) controller for the improvement of setpoint tracking or disturbance rejection responses and new tuning formulas for a FOPTD process model. The NPID controller has a structure with a first-order filter in the derivative term to avoid possible Derivative Kick. The parameters of the NPID controller are expressed in terms of the ratio L/τ of the time delay L to the time constant τ in the process by using the dimensionless approach. Repeated optimizations are performed for each value over the ranges of 0.01 to 1 and 1 to 3 of L/τ and over the ranges of 5 to 30 of the filter parameter N to obtain the average of optimal parameter values that minimize the integral of absolute error performance criterion. By using the least-squares method with together the calculated optimal values and the rule formulas, the tuning rules are obtained. A set of simulation works on the five processes are carried out to demonstrate tracking and disturbance performance and robustness against the noise of this approach.

Keywords Nonlinear PID controller · Tuning rules · FOPTD model · Genetic algorithms · CSTR

1 Introduction

During the past 70 years, the proportional-integral-derivative (PID) controller has been adopted in a variety of control loops due to its simplicity and usefulness (Ziegler and Nichols 1942; Ray 1989; Rivera et al. 1986; Åström et al. 1993; O’Dwyer 2006). Numerous modified versions of the standard form and their tuning methods have been proposed for improving the closed-loop response (O’Dwyer 2006). This improvement of the PID control technique has significantly impacted automation in the process industries.

The settings of a PID controller are mainly done in the time domain or the frequency domain. Some methods use information regarding the transient response of a step setpoint or the approximated model of a process. Other methods use some knowledge about the ultimate frequency values of a process. Although being initially well set, fixed-gain PID controllers often behave poorly due to process variations or uncertainties. For this reason, periodical retuning is required to maintain the desired closed-loop behavior. These shortcomings of PID controllers in dealing with complex process dynamics have resulted in challenges for research works on auto-tuning and self-tuning PID control that can deal effectively with a wide range of process control problems (Lee et al. 2017; Sun et al. 2020; Hernández-Alvarado et al. 2016; Pongfai et al. 2020; Ashida et al. 2017; Simorgh et al. 2020; Zhao and Xi 2020).

Lee et al. (2017) conducted a case study based on PID auto-tuning for the molten carbonate fuel cell (MCFC) operation framework. The tuning rules were computed based on the fractional-order plus time delay model. In

✉ Pikaso Pal
pikaso.iitism@gmail.com

¹ Department of Mechanical Facility Control Engineering, Korea University of Technology and Education, 1600 Chungjeol-ro, Dongnam-gu, Cheonan-si, Chungcheongnam-do, Korea

² Department of Electrical Power and Control Engineering, Adama Science and Technology University, P.O. Box 1888, Adama, Ethiopia

³ Department of Electrical Engineering, Indian Institute of Technology (Indian School of Mines), Dhanbad, Jharkhand, India

an automatic mechanical transmission system application, Sun et al. (2020) used a powertrain mathematical model to tune PID controller parameters automatically by minimizing the cost function in relationship with the outputs' tracking errors by incorporating the Nelder-Mead method. Based on neural networks, Hernández-Alvarado et al. (2016) implemented an auto-tune PID controller on remotely operated vehicles for trajectory tracking with unknown disturbances. Pongfai et al. (2020) designed a novel optimal PID auto-tuning controller based on a swarm learning process in which results were performed by comparing ant colony optimization with a new constrained Nelder-Mead algorithm, the genetic algorithm, the particle swarm optimization algorithm, and a neural network. Ashida et al. (2017) proposed a parameter tuning law for an implicit self-tuning PID control scheme to track the desired reference model output from the system output. In a highly nonlinear process such as a continuously stirred tank reactor (CSTR), Simorgh et al. (2020) designed a self-tuning PID controller using Ziegler-Nichols tuning algorithm based on online estimation methods by incorporating the noise, disturbance and variations in system dynamics. Zhao and Xi (2020) compared the manually tuning PID controller and the PID controller comprising the adaptive genetic algorithm.

Recently, to overcome the fixed-gain PID controller's poor performance, nonlinear PID control strategies using nonlinear functions to modify the structure of the conventional PID controller have been actively conducted (Seraji 1998, 1997; Han 2009; Guerrero et al. 2019; Hua et al. 2020). Seraji (1998, 1997) introduced a class of nonlinear PID controllers which consist of a nonlinear gain in cascade with a linear PID controller to scale the error. Han (2009) proposed a nonlinear PID controller with nonlinear gain functions combining $e(t)$, $\int e(t)dt$ and $\dot{e}(t)$ to achieve better tracking and noise rejection. An approach based on a novel nonlinear PID-type controller with an auto gain tuning mechanism was proposed by Guerrero et al. (2019) for a rotorcraft-based transportation system, which can achieve efficient payload positioning and aggressive maneuvering control. A decoupled nonlinear PID controller was developed via the Lyapunov design by Hua et al. (2020) for trajectory tracking control of an underwater vehicle, which proved the stability of the closed-loop system and improved robustness.

By the introduction of nonlinearities in their PID controller structure, the responses were successfully improved for some types of processes. Nevertheless, in most cases, the number of parameters to be tuned is greater than that of the standard PID controller, which causes difficulties in both tuning and implementation.

For this reason, the author introduced a nonlinear PID (NPID) controller that scales the error inputted by the integrator in the standard PID controller frame and the

setpoint tracking rules for the first-order plus time delay (FOPTD) model based on the Integral of Squared Error (ISE), the Integral of Absolute Error (IAE), and the Integral of Time multiply Absolute Error (ITAE) performance indices (Jin 2019). In this controller structure, the number of the tuning parameters is kept at 3, and the integrator wind-up can be partially prevented by scaling down large errors. Still, due to the use of the pure derivative term, there is a possibility that abrupt setpoint change or high-frequency noises will cause Derivative Kick.

In order to alleviate this limitation, we present an NPID controller that is of the form employed in industrial sites by supplementing the ideal derivative term with a first-order filter. Since many industrial processes can be approximated by the FOPTD model and PID controllers are usually tuned to fit for either setpoint tracking or disturbance rejection, we propose new tuning formulas for setpoint tracking and disturbance rejection for the NPID controller based on a genetic algorithm for optimization, and the least squares method for curve fitting. Three steps are here adopted. The first step involves using the dimensionless approach to express the parameters of the NPID controller in terms of the ratio L/τ of the time delay L to the time constant τ in the FOPDT process model. The second step produces the optimum NPID parameters to minimize the IAE performance criterion. Repeated optimizations are performed for different values of L/τ and N to obtain their averaged values. The last step obtains the tuning formulas using the least squares method with together the calculated values and the rule formulas.

The paper is organized as follows: Sect. 1 shows the direction of this study through a survey of existing methods. Section 2 gives a brief overview of the author's previous NPID controller and proposes an enhanced NPID controller. Section 3 obtains new tuning formulas for the NPID controller. Section 4 verifies the effectiveness of the proposed method through simulation of five processes, and finally, Sect. 5 offers concluding remarks.

2 Nonlinear PID controller

2.1 Structure of the NPID controller

NPID controller, which employs a nonlinear gain in cascade with the integral action of a conventional PID controller. Figure 1 shows the NPID control system. In Fig. 1, y_s denotes the setpoint, y the output (or the process variable) and u the control input, e the error between the setpoint and the output, v the scaled error, and $G_p(s)$ the process. (1)-(2) are the linear part transfer functions of the NPID controller, given by

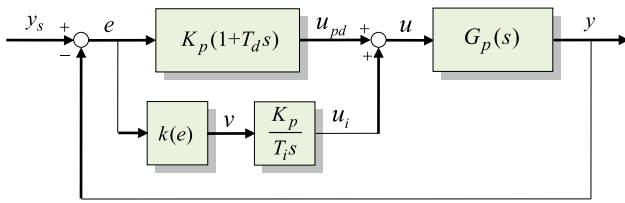


Fig. 1 The NPID control system

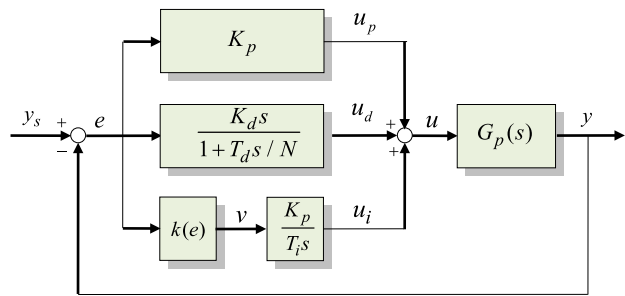


Fig. 2 The proposed NPID control system

$$\frac{U_{pd}}{E(s)} = K_p(1+T_d s) \tag{1}$$

$$\frac{U_i(s)}{V(s)} = \frac{K_p}{T_i s} \tag{2}$$

where K_p , T_i and T_d are the proportional gain, the integral time and the derivative time, respectively. The scaled error $v(t)$ in the integral term is described by

$$v(t) = k(e)e(t) \tag{3}$$

$k(e)$ is a nonlinear gain defined by

$$k(e) = \exp\left(-\frac{e^2}{2\sigma^2}\right) \tag{4}$$

where σ denotes the difference between the current setpoint value and the previous value in the step-type setpoint or does $dG_p(0)$ in the step-type disturbance d and $G_p(0)$ is the steady-state gain of the process.

The disadvantage of the ideal derivative term in (1) is that a sudden change in the setpoint or/and high-frequency noises coming into control loops will cause a phenomenon known as Derivative Kick. Due to this, in many field applications, PID controllers with a first-order filter in the derivative term are mainly adopted. In this paper, we propose an NPID controller, as shown in Fig. 2, which is an improvement of the NPID controller in Fig. 1.

The time-domain equation of the proposed NPID controller is given by

$$\begin{aligned} u(t) &= u_p(t) + u_i(t) + u_d(t), \\ u_p(t) &= K_p e(t), \\ u_i(t) &= \frac{K_p}{T_i} \int v(t) dt, \end{aligned} \tag{5}$$

$$\frac{T_d}{N} \frac{du_d(t)}{dt} + u_d(t) = K_p T_d \frac{de(t)}{dt}$$

where u_{pi} and u_d denote the PI action and the D action, respectively and N is a user-defined parameter. By using the approximation of a differentiator, the magnitude of its frequency $K_p T_d \omega / \sqrt{1 + T_d^2 \omega^2 / N^2}$ limited to NK_p as $\omega \rightarrow \infty$. This means that high-frequency measurement noise is amplified at most by a factor NK_p . N is appropriately selected according to the noise environment and typical values of N are 5 to 30 (O'Dwyer 2006; Åström et al. 1998).

The NPID controller given by (3)–(5) can be applied to linear and nonlinear processes, but many industrial processes can be approximated with the FOPTD model, i.e., a commonly used model. So we obtain new tuning rules based on the FOPTD process model given by

$$\tau \frac{dy(t)}{dt} + y(t) = Ku(t - L) \tag{6}$$

where K , τ , and L denote the steady-state gain, the time constant, and the time delay, respectively.

2.2 Dimensionless NPID control system

Defining dimensionless variable $t' = t/\tau$ and letting $u(\tau t') = \bar{u}(t')$, $e(\tau t') = \bar{e}(t')$ and $v(\tau t') = \bar{v}(t')$ to simplify the linear parts of the NPID controller in (5) gives

$$\begin{aligned} \bar{u}(t') &= \bar{u}_p(t') + \bar{u}_i(t') + \bar{u}_d(t'), \\ \bar{u}_p(t') &= K_p \bar{e}(t'), \\ \bar{u}_i(t') &= \frac{K_p \tau}{T_i} \int \bar{v}(t') dt', \\ \frac{T_d}{N\tau} \frac{d\bar{u}_d(t')}{dt'} + \bar{u}_d(t') &= \frac{K_p T_d}{\tau} \frac{d\bar{e}(t')}{dt'}. \end{aligned} \tag{7}$$

In a similar fashion, applying the dimensionless approach with defining $y(\tau t') = \bar{y}(t')$ to (6) yields

$$\frac{d\bar{y}(t')}{dt'} + \bar{y}(t') = K\bar{u}\left(t' - \frac{L}{\tau}\right) \tag{8}$$

(7) and (8) can be expressed in the form of the transfer function as

$$\bar{U}(s) = K_p [\bar{E}(s) + \frac{1}{T_i s} \bar{V}(s) + \frac{\bar{T}_d s}{1 + \frac{\bar{T}_d}{N} s} \bar{E}(s)] \tag{9}$$

$$\frac{\bar{Y}(s)}{\bar{U}(s)} = \frac{Ke^{-\bar{L}s}}{s+1} \tag{10}$$

where $\bar{T}_i = T_i/\tau$, $\bar{T}_d = T_d/\tau$, and $\bar{L} = L/\tau$.

Combining the process gain K with the proportional gain K_p of the NPID controller and applying a disturbance on the input side yields the block diagram of the dimensionless NPID control system. By doing this, the number of process parameters becomes only one, and the tuning parameters KK_p , \bar{T}_i and \bar{T}_d of the NPID controller become functions of $\bar{L} = L/\tau$.

3 Tuning formulas of the NPID controller

3.1 Performance Index

When tuning one degree of freedom PID controllers, it is difficult to simultaneously achieve good transient behavior toward changes in setpoint and an appropriate reduction of disturbances. The following shows an example of this. With $K=1$, $\tau=1$, $L=1$, and $N=10$ in Fig. 2, the result of applying a non dominated sorting genetic algorithm (NSGA-II) to the multiobjective problem of minimizing a setpoint tracking performance index and another disturbance rejection performance index is shown in Fig. 3. It can be seen from the optimal Pareto front in Fig. 3 and responses in Fig. 4 that are tuning for good setpoint tracking degrades disturbance rejection, whereas tuning for fast disturbance rejection results in poor setpoint tracking. Therefore, they are usually tuned to fit for either setpoint tracking or disturbance rejection, depending on the purpose of long-term use.

As seen in Fig. 5 with a choice of N , the NPID controller has three tuning parameters tuning parameters KK_p , $\bar{T}_i (= T_i/\tau)$ and $\bar{T}_d (= T_d/\tau)$ functions of $\bar{L} (= L/\tau)$. Finding

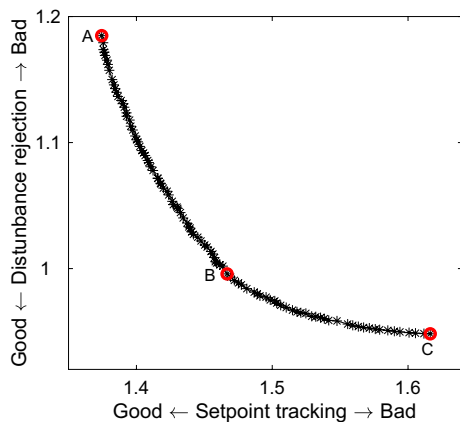


Fig. 3 Optimal Pareto front

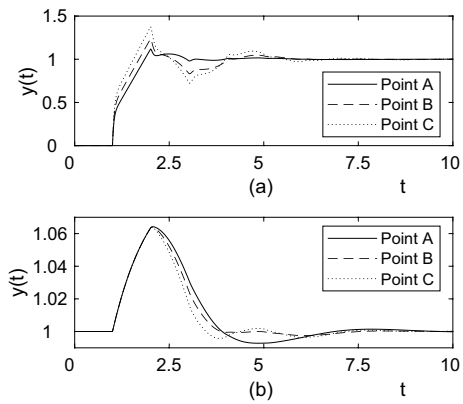


Fig. 4 Responses at three points on optimal Pareto front

tuning formulas for the FOPTD process model provides the smallest overshoot, fastest rise time, or quickest settling time leads to optimization problems. Applying a GA to these optimization problems is one of the most challenging steps and requires the design of objective functions. In order to combine all of these objectives, we use a single performance index in terms of the integral of the absolute value of the error (IAE) as

$$IAE = \int_0^\infty |y_s(t') - \bar{y}(t')| dt' \tag{11}$$

where $\bar{y}(t')$ is the output of the dimensionless system.

3.2 Optimum parameters

The average of 20 repeated calculations was performed for each value over the ranges of 0.01 to 1 and 1 to 3 of L/τ and over the ranges of 5 to 30 of N to obtain a set of optimal parameters that minimize IAE and was plotted in Fig. 6 for setpoint tracking and Fig. 7 for disturbance rejection, respectively. The points marked ‘○’ in the figures denote the averaged results.

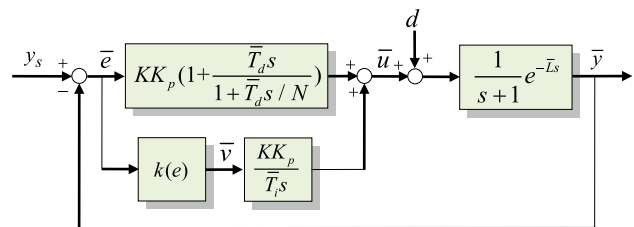
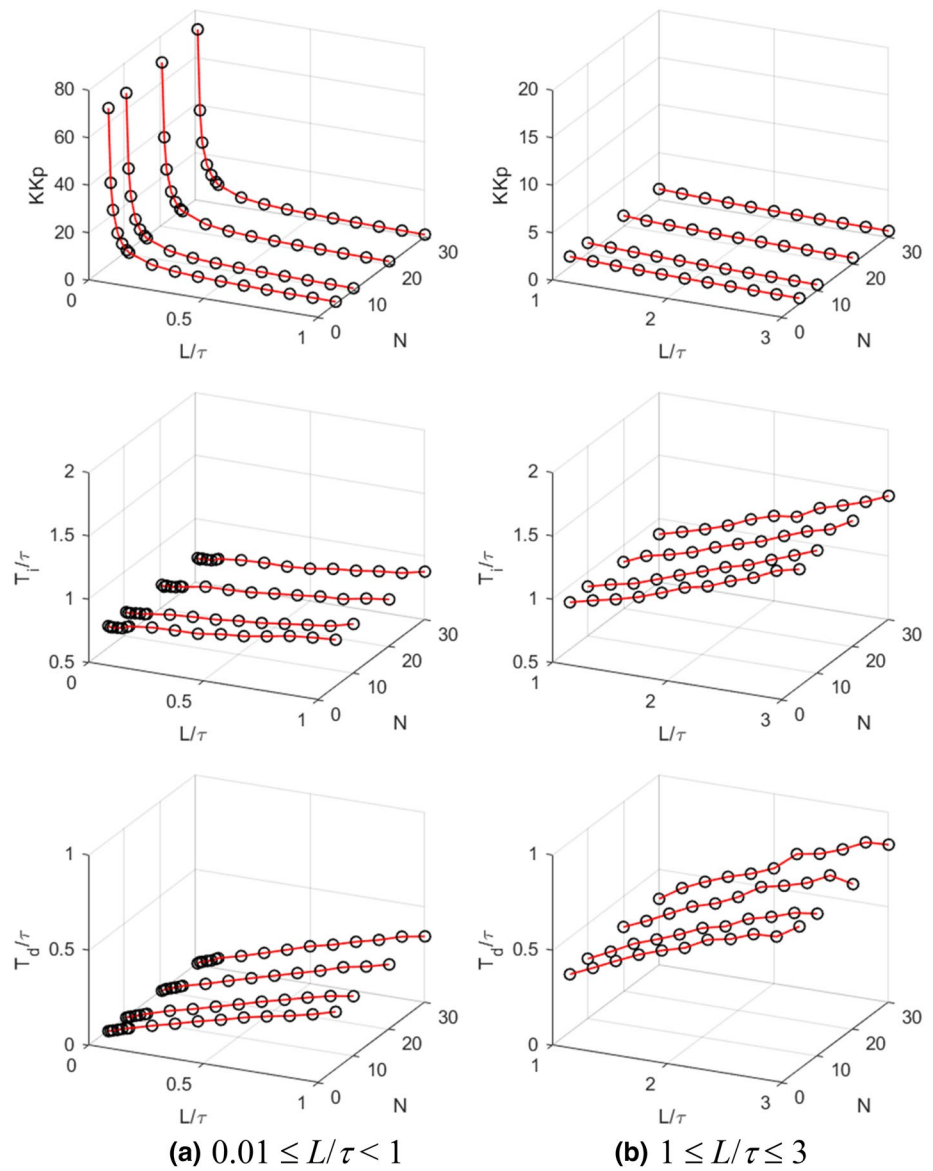


Fig. 5 Dimensionless NPID control system

Fig. 6 Optimal parameter values for setpoint tracking



3.3 Tuning rule formulas

With the optimally calculated values, the following empirical formulas of the form used in O’Dwyer (2006), Zhuang and Atherton (1993) were adopted as the models of the curve fitting.

$$K_p = a_1 \left(\frac{L}{\tau}\right)^{b_1}, \frac{T_i}{\tau} = a_2 + b_2 \left(\frac{L}{\tau}\right) \tag{12}$$

and $\frac{T_d}{\tau} = a_3 \left(\frac{L}{\tau}\right)^{b_3}$ for setpoint tracking

$$K_p = a_1 \left(\frac{L}{\tau}\right)^{b_1}, \frac{T_i}{\tau} = a_2 \left(\frac{L}{\tau}\right)^{b_2} \tag{13}$$

and $\frac{T_d}{\tau} = a_3 \left(\frac{L}{\tau}\right)^{b_3}$ for disturbance rejection

By using the least squares method, the parameters of these formulas over the given ranges of L/τ and N were obtained for setpoint tracking and disturbance rejection and listed in Tables 1, 2, 3, 4, respectively.

Figures 8–9 show the 3D surfaces of the interpolated tuning rules combining Table 1 with Table 2, and Table 3 with Table 4, respectively. The figures imply that there are differences to some extent for N , but not large.

Fig. 7 Optimal parameter values for disturbance rejection

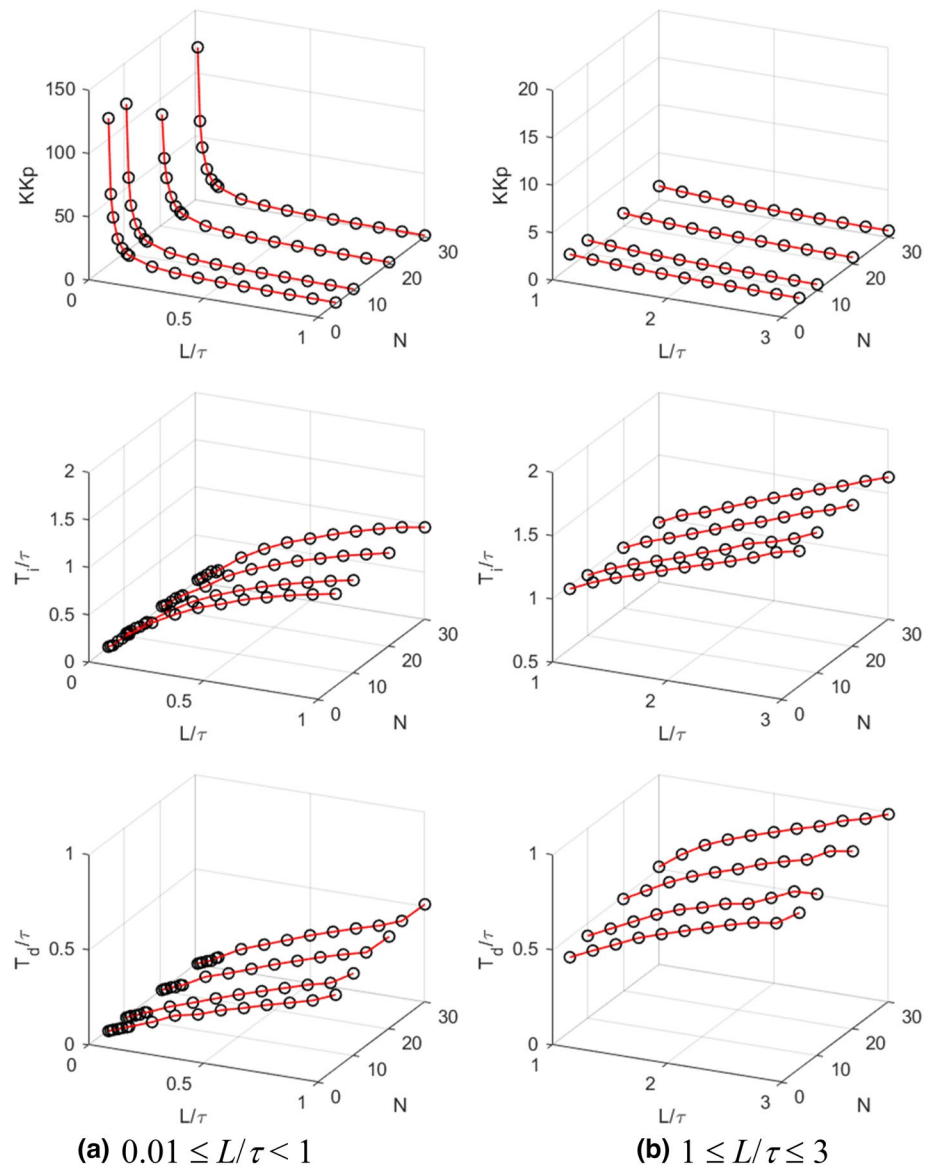


Table 1 NPID controller tuning rules for setpoint tracking ($0.01 \leq L/\tau < 1$)

N	Dimensionless parameters		
	KK_p	T_i/τ	T_d/τ
5	$0.9581\left(\frac{L}{\tau}\right)^{-0.9141}$	$0.6790 + 0.1889\frac{L}{\tau}$	$0.2948\left(\frac{L}{\tau}\right)^{0.8749}$
10	$1.0103\left(\frac{L}{\tau}\right)^{-0.9035}$	$0.6845 + 0.1686\frac{L}{\tau}$	$0.3141\left(\frac{L}{\tau}\right)^{0.8540}$
20	$1.0246\left(\frac{L}{\tau}\right)^{-0.9065}$	$0.6854 + 0.1714\frac{L}{\tau}$	$0.3305\left(\frac{L}{\tau}\right)^{0.8352}$
30	$1.0360\left(\frac{L}{\tau}\right)^{-0.9058}$	$0.6886 + 0.1601\frac{L}{\tau}$	$0.3294\left(\frac{L}{\tau}\right)^{0.7878}$

Table 2 NPID controller tuning rules for setpoint tracking ($1 \leq L/\tau < 3$)

N	Dimensionless parameters		
	KK_p	T_i/τ	T_d/τ
5	$1.0625\left(\frac{L}{\tau}\right)^{-0.4857}$	$0.5593 + 0.2867\frac{L}{\tau}$	$0.3105\left(\frac{L}{\tau}\right)^{0.8029}$
10	$1.0901\left(\frac{L}{\tau}\right)^{-0.4830}$	$0.5743 + 0.2931\frac{L}{\tau}$	$0.3229\left(\frac{L}{\tau}\right)^{0.7971}$
20	$1.1161\left(\frac{L}{\tau}\right)^{-0.4903}$	$0.5699 + 0.2985\frac{L}{\tau}$	$0.3442\left(\frac{L}{\tau}\right)^{0.7846}$
30	$1.1261\left(\frac{L}{\tau}\right)^{-0.4849}$	$0.5670 + 0.2987\frac{L}{\tau}$	$0.3573\left(\frac{L}{\tau}\right)^{0.7956}$

Table 3 NPID controller tuning rules for disturbance rejection ($0.01 \leq L/\tau < 1$)

N	Dimensionless parameters		
	KK_p	T_i/τ	T_d/τ
5	$1.2472 \left(\frac{L}{\tau}\right)^{-0.9796}$	$1.1409 \left(\frac{L}{\tau}\right)^{0.8224}$	$0.4024 \left(\frac{L}{\tau}\right)^{0.9638}$
10	$1.3239 \left(\frac{L}{\tau}\right)^{-0.9714}$	$1.1091 \left(\frac{L}{\tau}\right)^{0.8101}$	$0.4304 \left(\frac{L}{\tau}\right)^{0.9578}$
20	$1.4159 \left(\frac{L}{\tau}\right)^{-0.9322}$	$1.0958 \left(\frac{L}{\tau}\right)^{0.8076}$	$0.4362 \left(\frac{L}{\tau}\right)^{0.8821}$
30	$1.3829 \left(\frac{L}{\tau}\right)^{-0.9718}$	$1.1008 \left(\frac{L}{\tau}\right)^{0.8189}$	$0.4806 \left(\frac{L}{\tau}\right)^{0.9489}$

Table 4 NPID controller tuning rules for disturbance rejection ($1 \leq L/\tau < 3$)

N	Dimensionless parameters		
	KK_p	T_i/τ	T_d/τ
5	$1.2612 \left(\frac{L}{\tau}\right)^{-0.6358}$	$0.9673 \left(\frac{L}{\tau}\right)^{0.4300}$	$0.3979 \left(\frac{L}{\tau}\right)^{0.6449}$
10	$1.3396 \left(\frac{L}{\tau}\right)^{-0.6479}$	$0.9654 \left(\frac{L}{\tau}\right)^{0.4455}$	$0.4415 \left(\frac{L}{\tau}\right)^{0.6138}$
20	$1.3681 \left(\frac{L}{\tau}\right)^{-0.6479}$	$0.9662 \left(\frac{L}{\tau}\right)^{0.4515}$	$0.4950 \left(\frac{L}{\tau}\right)^{0.5839}$
30	$1.3891 \left(\frac{L}{\tau}\right)^{-0.6579}$	$0.9580 \left(\frac{L}{\tau}\right)^{0.4659}$	$0.5365 \left(\frac{L}{\tau}\right)^{0.5594}$

4 Simulation results

The objective of simulation works on five processes including a nonlinear CSTR process is to compare the responses of the proposed method with those of the PID controllers proposed by the Lopez setting (hereafter referred to as PID-Lopez) (Lopez and Murril 1967) and the CHR setting

(hereafter referred to as PID-CHR) (Chien et al. 1972). In the case of the CSTR process, the response of the proposed method is compared with that of the adaptive controller proposed by Chen and Peng (1999) (hereafter referred to as AC-Chen). *N* is set to 10 for the NPID controller.

4.1 Case 1: FOPTD processes

The transfer functions of the FOPTD processes are given by

$$G_{p1}(s) = \frac{e^{-5s}}{1 + 10s} \tag{14}$$

$$G_{p2}(s) = \frac{e^{-10s}}{1 + 10s} \tag{15}$$

$$G_{p3}(s) = \frac{e^{-20s}}{1 + 10s} \tag{16}$$

The ratio L/τ of the time delay to the time constant in each process $G_{p1}(s)$, $G_{p2}(s)$, and $G_{p3}(s)$ is 0.5, 1, and 2, respectively. The controller settings for these three processes using the PID-Lopez method, the PID-CHR method and the proposed method are summarized in Table 5. The responses for unit step changes in setpoint or disturbance using these settings are plotted in Figs. 10, 11, 12.

In order to assess the performance of the three methods quantitatively, rise time $t_r = t_{95} - t_5$, overshoot M_p , 2% settling time t_s , and the integral of absolute error $IAE = \int_0^\infty |e(t)| dt$ were obtained for setpoint tracking and perturbation peak M_{peak} , recovery time t_{rcy} and IAE for disturbance rejection. M_{peak} denotes $|y_{max} - y_s|$ or $|y_{min} - y_s|$ and t_{rcy} does the time that it takes for y to recover within 2% of y_s . It is evident in the figures that the responses are faster when using the NPID controller, without a significant increase of the overshoot and settling time. More precisely, compared with the other methods in Table 6, t_r of the NPID controller is smaller

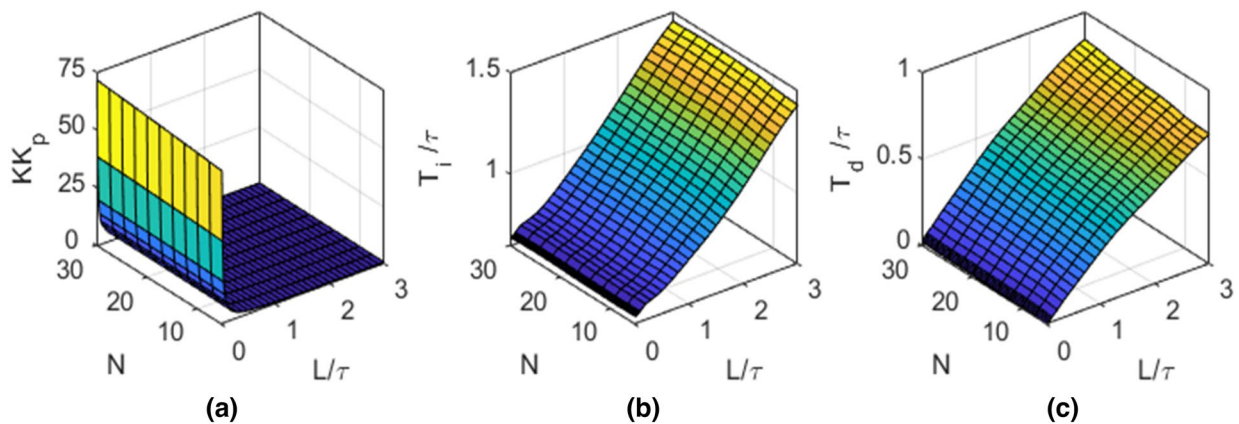


Fig. 8 Tuning rule surfaces for setpoint tracking: **a** KK_p versus L/τ and N ; **b** T_i/τ versus L/τ and N ; **c** T_d/τ versus L/τ and N

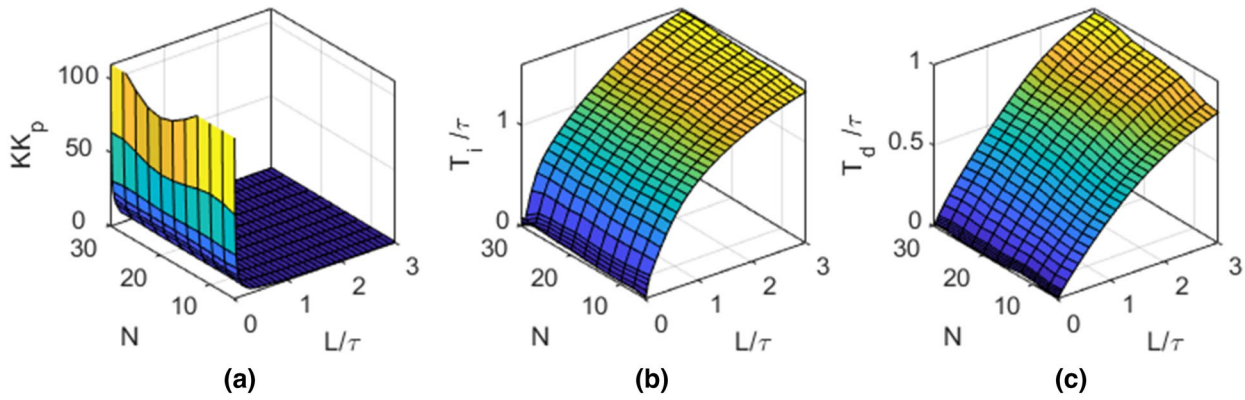


Fig. 9 Tuning rule surfaces for disturbance rejection: a KK_p versus L/τ and N ; b T_i/τ versus L/τ and N ; c T_d/τ versus L/τ and N

Table 5 Settings for setpoint tracking and disturbance rejection on Processes 1–3

Process	Tuning Method	Setpoint tracking			Disturbance rejection		
		K_p	K_i	K_d	K_p	K_i	K_d
1	PID-Lopez	1.739	0.126	2.796	2.616	0.367	5.001
	PID-CHR	1.900	0.136	4.465	2.400	0.240	5.040
	NPID-Proposed	1.890	0.246	3.284	2.596	0.410	5.752
2	PID-Lopez	0.965	0.063	2.953	1.357	0.114	5.170
	PID-CHR	0.950	0.068	4.465	1.200	0.060	5.040
	NPID-Proposed	1.090	0.126	3.520	1.339	0.139	5.914
3	PID-Lopez	0.535	0.027	3.119	0.704	0.036	5.345
	PID-CHR	0.475	0.034	4.465	0.600	0.015	5.040
	NPID-Proposed	0.780	0.067	4.376	0.855	0.065	5.776

while IAE is least, and both M_p and t_s are reasonable in the case of setpoint tracking. Both the PID-Lopez method and the proposed method give better closed-loop responses with smaller IAE and shorter t_{rcy} . In contrast, the PID-CHR method yields sluggish disturbance rejection performances with larger IAE and longer t_{rcy} .

4.2 Case 2: Fourth-order process

Consider a 4th-order process used in Åström et al. (1998):

$$G_{p4}(s) = \frac{0.36(1 - s)e^{-s}}{(12s + 1)(3s + 1)(0.2s + 1)(0.05s + 1)} \tag{17}$$

There are several parameter estimation techniques for approximating the 4th-order process to a FOPTD model (Skogestad 2004; Young 1981). The estimates of the FOPTD model are $K=0.36$, $\tau=12.28$, and $L=5.20$. These values were used for the settings of the PID controller and (17) was used for the NPID controller tuning and simulation. Controller settings are summarized in Table 7. Figure 13 shows a comparison of the unit step responses of the PID and NPID control systems. It is seen in Fig. 13 that the response of the

NPID controller is clearly better than those of the others. Tables 8 and 9 list the quantitative results obtained from simulation.

4.3 Case 3: CSTR process

Consider a CSTR model used in Chen and Peng (1999). The mathematical model is given by

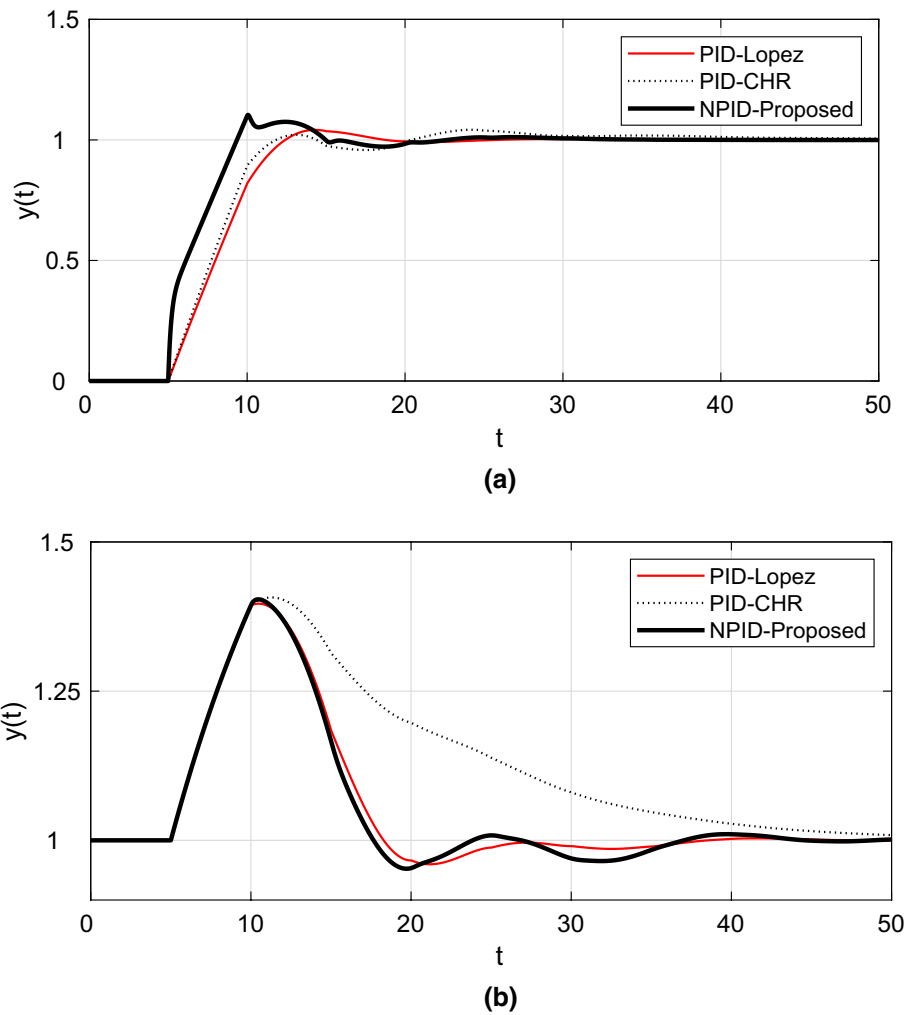
$$\dot{x}_1 = -x_1 + D_a(1 - x_1) \exp\left(\frac{x_2}{1 + x_2/\gamma}\right) + d_1, \tag{18a}$$

$$\dot{x}_2 = -(1 + \beta)x_2 + HD_a(1 - x_1) \exp\left(\frac{x_2}{1 + x_2/\gamma}\right) + \beta u + d_2, \tag{18b}$$

$$y = x_2, \tag{18c}$$

where x_1 and x_2 are the concentration C and the temperature T , respectively; y and u are the outlet temperature of the reactant and the temperature of cooling water, respectively; d_1 and d_2 disturbances; D_a is the Damökhler number; H is the heat of reaction; β the heat transfer coefficient; $\gamma = E/RT_f$

Fig. 10 Unit step responses of the three methods on Process 1: **a** setpoint **b** disturbance



E activation energy [cal/mol]; and R is the gas constant [cal/mol–K]. $x_1, x_2, u,$ and t are non-dimensionalized by

$$x_1 = \frac{C_f - C}{C_f}, x_2 = \frac{T - T_f}{T_f} \gamma, u = \frac{T_c - T_f}{T_f} \gamma, t = t' \frac{F_f}{V}. \quad (19)$$

where C_f, T_f, F_f and C, T, F denote the concentration [mol/m³], temperature [K], and flow [m³/sec] at the inlet and outlet of the reactant, respectively. T_{cf}, F_{cf} and T_c, F_c are the temperature and flow at the inlet and outlet of cooling water, respectively. V is the volume of the CSTR [m³]. The open-loop process has nominal values $D_a = 0.072, \gamma = 20, H = 8,$ and $\beta = 0.3$ (Chen and Peng 1999). With these nominal values, the process has two stable equilibrium points $x_a = [0.144, 0.886]^T$ and $x_c = [0.765, 4.705]^T$, and one unstable equilibrium point $x_b = [0.447, 2.752]^T$.

In the case of an exothermic reaction, a coolant stream needs to be passed through the cooling jacket to remove the extra heat and maintain the reaction temperature. As the flow-changing valve operation as a control input for controlling the outlet temperature T_c of the jacket has a physical

limit, the input saturation is limited between $u_{min} = -5$ and $u_{max} = 5$. In the case of the AC-Chen method, the parameters $\eta = 0.2, m = 5,$ and $\text{sign}(\partial y/\partial x) = 1$ were used for the adaptive controller.

4.3.1 Setpoint tracking response

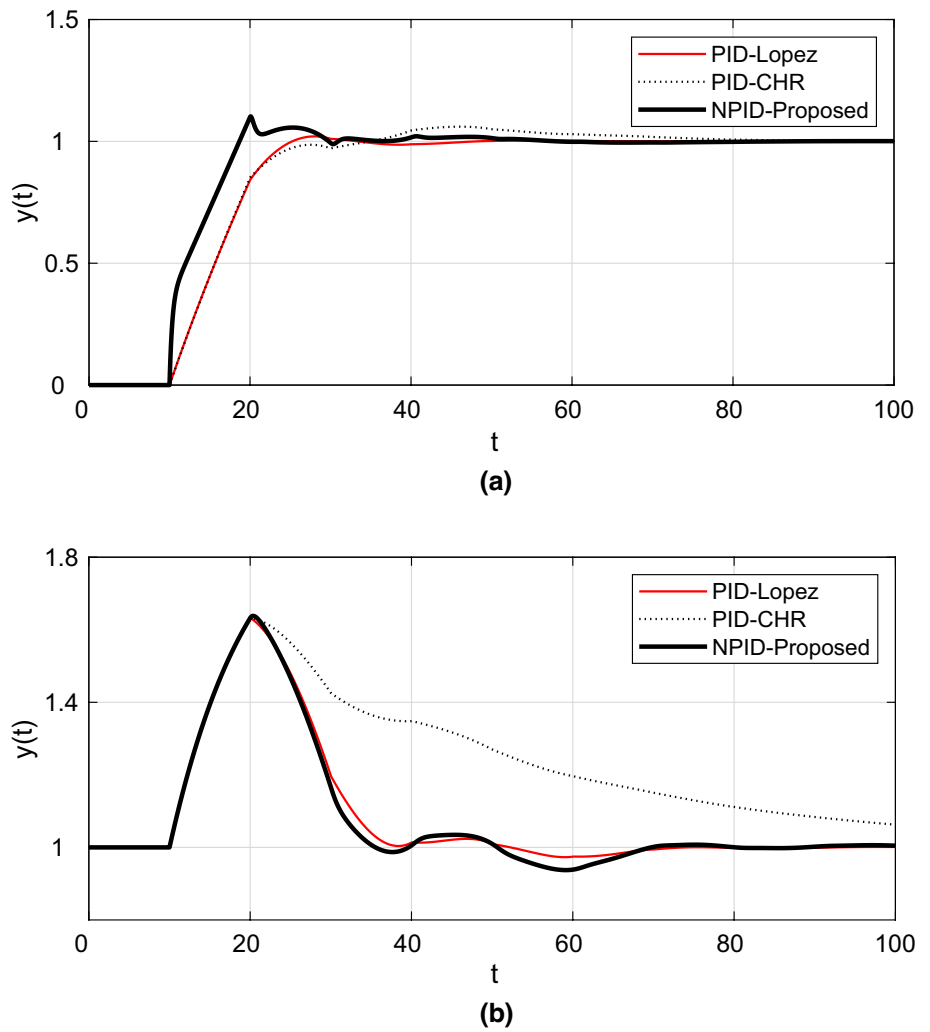
Since the CSTR process in (18) is highly nonlinear, the NPID controller was directly tuned using a GA while step setpoint signals were changed from 0.886 to 2.752 at $t = 1$ and from 2.752 to 4.705 at $t = 16$ and vice versa, as shown in Fig. 14. This tuning results in the settings $K_p = 91.056, K_i = 0.026$ and $K_d = 11.561$ for setpoint tracking.

Again, it is seen that the response of the proposed method is better than that of the AC-Chen method. Table 5, which summarizes the quantitative results, also proves this.

4.3.2 Disturbance rejection response

The settings of the NPID controller were obtained in a similar manner while applying step disturbances $d_1 = 0.2, d_2 = 0.2$

Fig. 11 Unit step responses of the three methods on Process 2: a setpoint b disturbance



at $t=1$ and then $d_1 = -0.2$, $d_2 = -0.2$ at $t=16$ with constant y_s of 2.752. The results are $K_p = 64.997$, $K_i = 129.999$ and $K_d = 20.002$ for disturbance rejection. The response of the proposed method is shown in Fig. 15, together with that of the AC-Chen method.

From Fig. 15 and Table 10, it is seen that M_{peak} , t_{rcy} and IAE of the proposed method are better than those of the AC-Chen method.

4.3.3 Noise elimination response

In order to validate the robustness of the proposed method against noise, a Gaussian noise $N(0,0.03^2)$ equivalent to about 15% of the change in the setpoint value was applied to the output stage. Figure 16 shows the responses of the two methods.

Comparing Fig. 16 with Fig. 14(a) without noise, the proposed method shows a satisfactory response even in a noisy environment.

5 Conclusion

This paper has proposed an enhanced NPID controller to improve setpoint tracking or disturbance rejection responses and avoid possible *Derivative Kick*. The parameters of the NPID controller were expressed in terms of L/τ using the dimensionless approach. Repeated optimizations of 20 were performed for each value over the ranges of 0.01 to 1 and 1 to 3 of L/τ and over the ranges of 5 to 30 of N to obtain the averaged parameter values that minimize the IAE criterion. By using the least-squares method with together the calculated values and the rule formulae, the new tuning rules have been obtained. A set of simulation works on the five processes have depicted that the proposed method demonstrated good tracking and disturbance performance and robustness against noise well than the other methods. The proposed method worked well for particularly the higher-order process and the non-linear process. In future works, the proposed rules can be applied to an auto-tuning approach.

Fig. 12 Unit step responses of the three methods on Process 3: **a** setpoint **b** disturbance

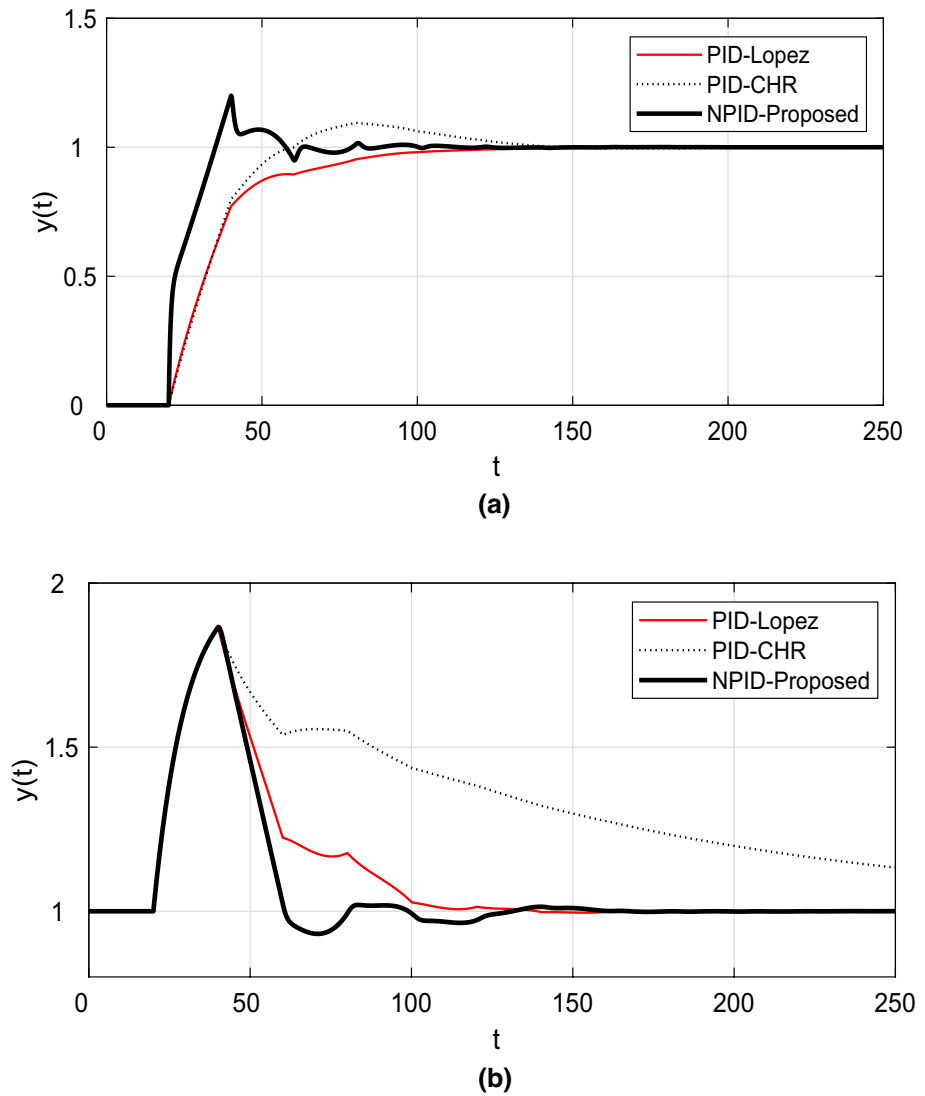


Table 6 Performance comparison of the three methods on Processes 1–3

Process	Tuning method	Setpoint tracking				Disturbance rejection		
		t_r	M_p	t_s	IAE	M_{peak}	t_{rcy}	IAE
1	PID-Lopez	6.226	4.175	16.960	8.331	0.397	35.846	3.320
	PID-CHR	5.514	4.219	28.688	8.533	0.407	> 50	6.242
	NPID-Proposed	4.002	10.355	19.766	7.044	0.404	41.609	3.348
2	PID-Lopez	12.388	2.049	28.471	8.112	0.633	66.947	4.709
	PID-CHR	13.127	6.031	68.887	8.813	0.633	> 100	11.551
	NPID-Proposed	7.971	10.238	40.976	6.905	0.638	67.631	4.816
3	PID-Lopez	58.384	–	98.206	7.417	0.865	105.630	5.675
	PID-CHR	30.503	9.475	125.706	7.498	0.865	> 250	16.919
	NPID-Proposed	13.666	19.962	74.509	5.331	0.866	122.271	4.562

Table 7 Controller settings for Process 4

Tuning method	Setpoint tracking			Disturbance rejection		
	K_p	K_i	K_d	K_p	K_i	K_d
PID-Lopez	5.565	0.333	9.412	8.505	1.100	16.923
PID-CHR	3.936	0.321	10.233	6.232	0.499	13.610
NPID-Proposed	9.495	0.952	24.315	17.094	3.175	40.362

Fig. 13 Unit step responses of the three methods on Process 4: **a** setpoint **b** disturbance

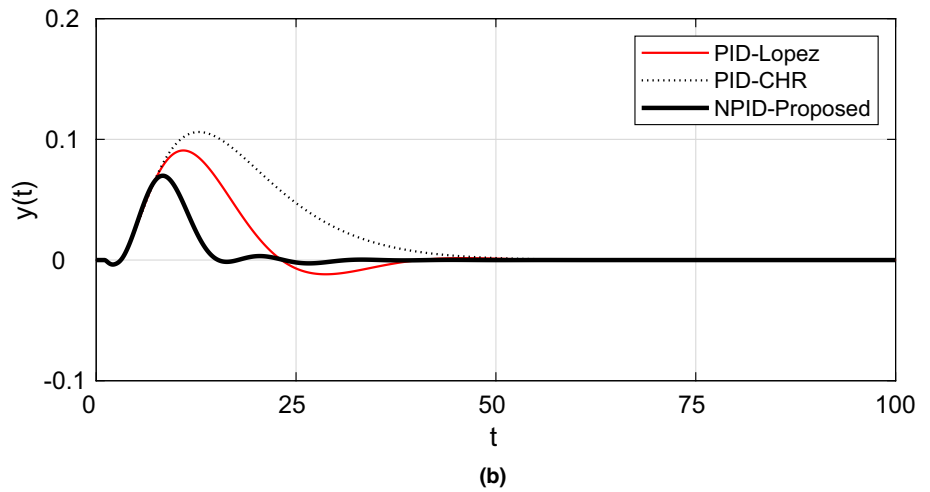
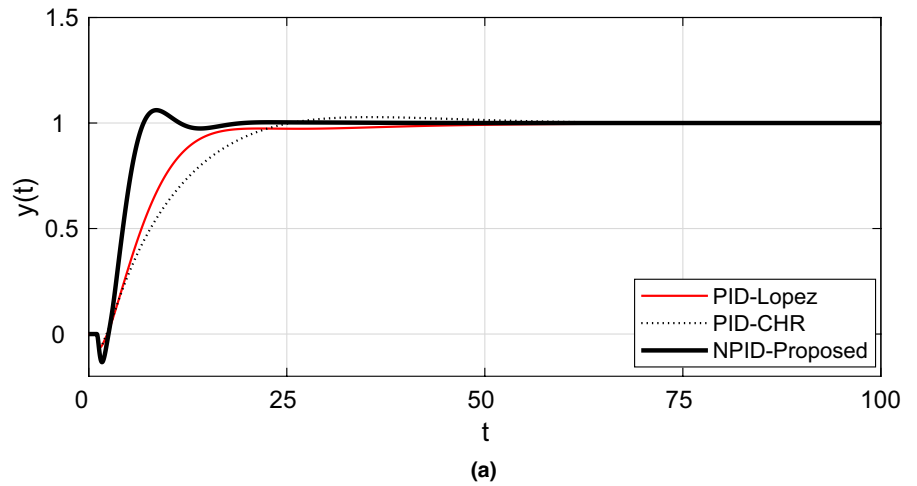


Table 8 Performance comparison of the three methods on Process 4

Tuning Method	Setpoint tracking				Disturbance rejection		
	t_r	M_p	t_s	IAE	M_{peak}	t_{rcy}	IAE
PID-Lopez	12.783	–	34.951	8.345	0.091	38.241	1.159
PID-CHR	17.952	2.794	44.026	9.967	0.106	48.377	2.012
NPID-Proposed	3.712	6.088	15.216	4.859	0.068	33.436	0.486

Table 9 Performance comparison of the two methods on the CSTR process

Setpoint	Method	$y_s = 0.886 \rightarrow 2.752$				$y_s = 2.752 \rightarrow 4.705$			
		t_r	M_p	t_s	IAE	t_r	M_p	t_s	IAE
Up	AC-Chen	1.053	13.167	3.386	1.373	0.606	32.050	2.392	1.397
	NPID-Proposed	1.026	1.082	1.163	1.136	0.649	4.482	1.111	1.033
Down	AC-Chen	0.807	9.371	2.976	1.098	0.983	3.324	2.079	1.200
	NPID-Proposed	0.797	0.927	0.934	0.922	0.921	0	1.113	1.145

Fig. 14 Step responses of the two methods for changes in setpoint: **a** $y_s = 0.886 \rightarrow 2.752 \rightarrow 4.705$, **b** $y_s = 4.705 \rightarrow 2.752 \rightarrow 0.886$.

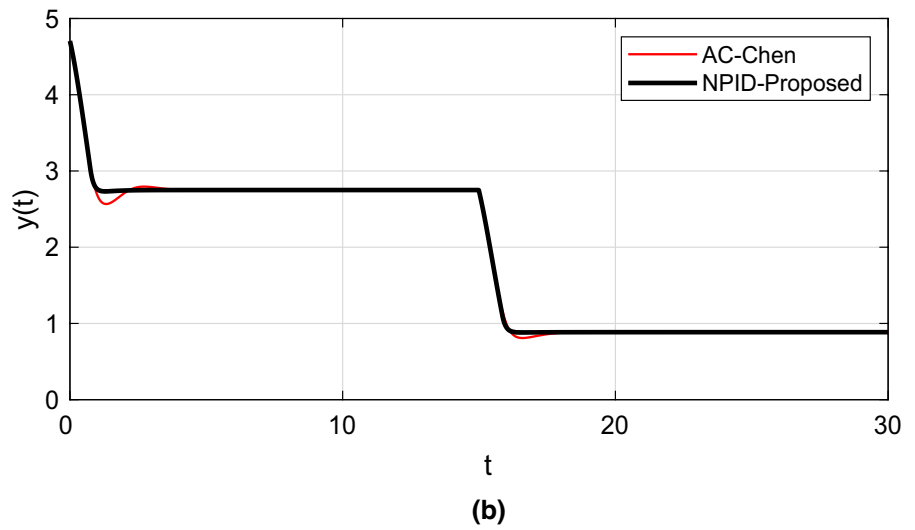
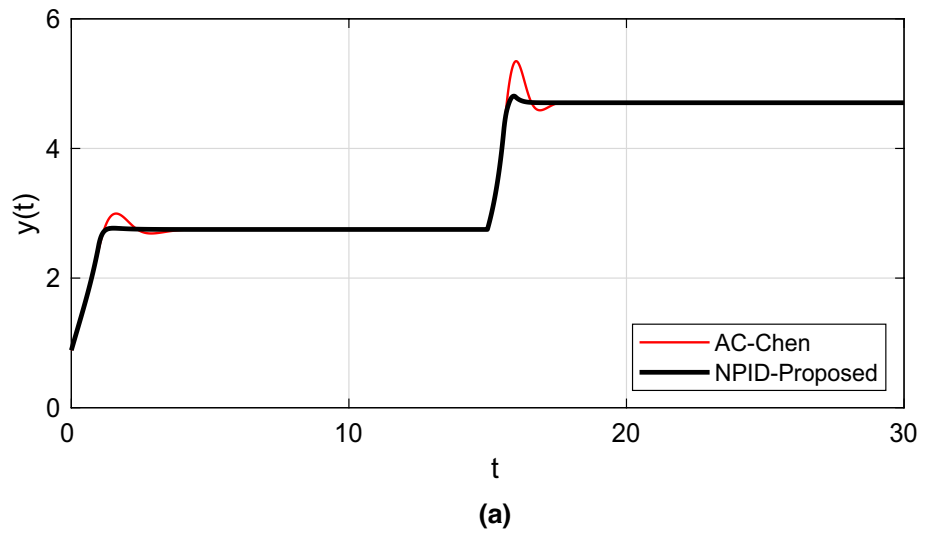


Fig. 15 Responses of the two methods for changes in disturbances on the CSTR process

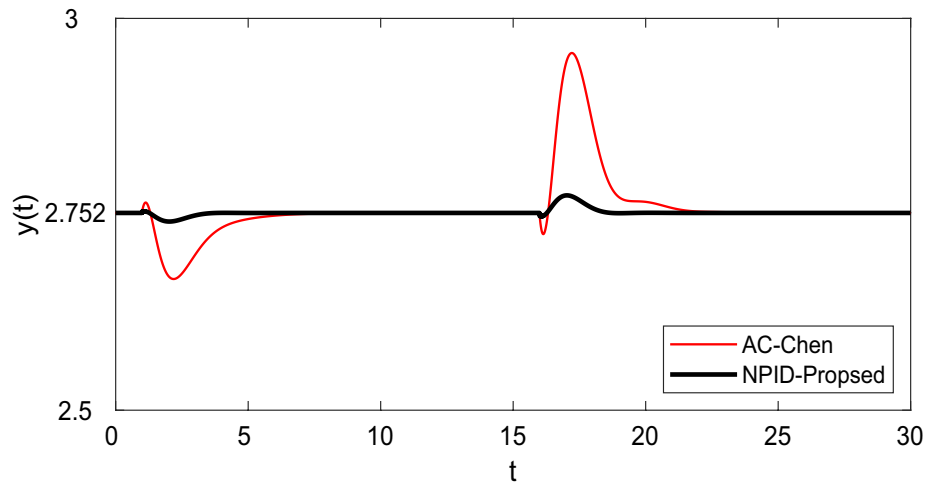
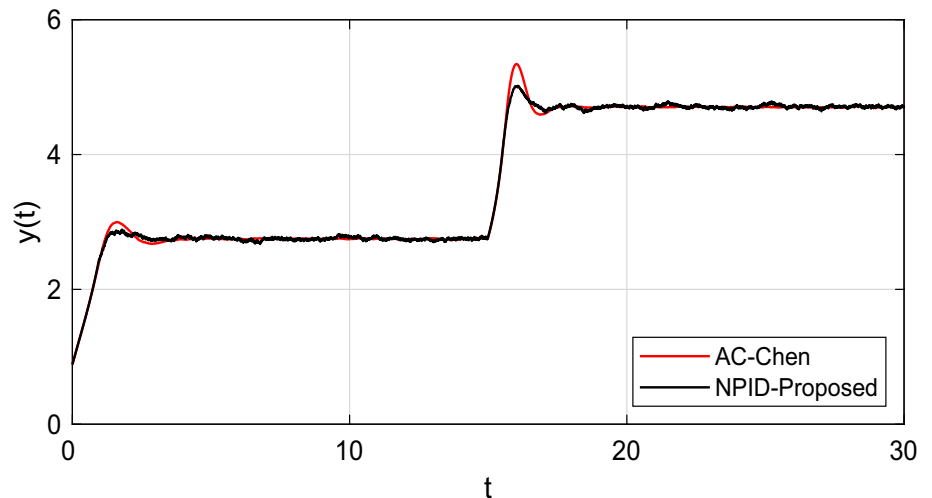


Table 10 Performance comparison of the two methods on the CSTR process

Method	$d_1=0.2$ and $d_2=0.2$			$d_1=-0.2$ and $d_2=-0.2$		
	M_{peak}	t_{rcy}	IAE	M_{peak}	t_{rcy}	IAE
AC-Chen	0.0843	6.8450	0.1647	0.2038	5.2878	0.3405
NPID-Proposed	0.0110	3.6519	0.0141	0.0222	3.3443	0.0304

Fig. 16 Step responses of the two methods under noise



Funding No funding available.

Declarations

Conflict of interest The Author(s) declare(s) that there is no conflict of interest.

Human participants and/or animals Not applicable.

Informed consent Not applicable.

References

Ashida Y, Wakitani S, Yamamoto T (2017) Design of an implicit self-tuning PID controller based on the generalized output. IFAC-Papers OnLine 50(1):13946–13951

Åström KJ, Hägglund T, Hang CC, Ho WK (1993) Automatic tuning and adaptation for PID controllers: a survey. Control Eng Practice 1(4):699–714

Åström KJ, Panagopoulos H, Hägglund T (1998) Design of PI controllers based on non-convex optimization. Automatica 34(5):585–601

- Chen CT, Peng ST (1999) Learning control of process systems with hard input constraints. *J Process Control* 9(2):151–160
- Chien KL, Hrones JA, Reswick JB (1972) On the automatic control of generalized passive systems. *Trans ASME* 74:175–185
- GG Jin, YD Son (2019) Design of a nonlinear PID controller and tuning rules for first-order plus time delay models. *Stud Inform Control* 28(2):157–166
- Guerrero J, Torres J, Creuze V, Chemori A, Campos E (2019) Saturation based nonlinear PID control for underwater vehicles: design, stability analysis and experiments. *Mechatronics* 61:96–105
- Han J (2009) From PID to active disturbance rejection control. *IEEE Trans Industr Electron* 56(3):900–906
- Hernández-Alvarado R, García-Valdovinos LG, Salgado-Jiménez T, Gómez-Espinosa A, Fonseca-Navarro F (2016) Neural network-based self-tuning PID control for underwater vehicles sensors. *MDPI J/sensors* 16(19):1429–1447
- Hua H, Fang Y, Zhang X, Qian C (2020) Auto-tuning nonlinear PID-type controller for rotorcraft-based aggressive transportation. *Mech Syst Signal Process* 145:106858
- Lee D, Cheon Y, Ryu JH, Lee IB (2017) An MCFC operation optimization strategy based on PID auto-tuning control. *Int J of Hydrogen Energy* 42(40):25518–25530
- Lopez AM, Murril PW (1967) Tuning controllers with error-integral criteria. *Instrum Technol* 14:57–62
- O'Dwyer A, (2006) *Handbook of PI and PID Controller Tuning Rules*, Second Ed. Imperial College Press, pp. 154–180
- Pongfai J, Su X, Zhang H, Assawinchaichote W (2020) A novel optimal PID controller autotuning design based on the SLP algorithm. *Expert Syst* 37(2):e12489
- Ray WH (1989) *Advanced Process Control*, 3rd edn. Butterworth Publishers, London
- Rivera DE, Morari M, Skogestad S (1986) Internal model control: PID controller design. *Ind Eng Chem Process Des Dev* 25(5):252–265
- Seraji H (1997) A new class of nonlinear PID controllers. In: *Proceedings of the 5th IFAC Symposium on Robot Control 1997 (SYROCO '97)*, Nantes, France, pp. 65–71
- Seraji H (1998) A new class of nonlinear PID controllers with robotic applications. *J Robot Syst* 15(3):161–181
- Simorgh A, Razminia A, Shiryaev VI (2020) System identification and control design of a nonlinear continuously stirred tank reactor. *Math Comput Simul* 173:16–31
- Skogestad S (2004) Simple analytic rules for model reduction and PID controller tuning. *MIC---Model Identif Control* 25(2):85–120
- Sun Z, Sanada K, Gao B, Jin J, Fu J, Huang L, Wu X (2020) Improved decoupling control for a powershift automatic mechanical transmission employing a model-based PID parameter autotuning method. *MDPI J/actuators* 9(3):54–75
- Young P (1981) Parameter estimation for continuous-time models—A survey. *Automatica* 17(1):23–39
- Zhao J, Xi M (2020) Self-tuning of PID parameters based on adaptive genetic Algorithm. *2020 IOP Conf Ser Mater Sci Eng*.782:042028.
- Zhuang M, Atherton DP (1993) Automatic tuning of optimum PID controllers. *IEE Proc-D* 140(3):216–224
- Ziegler JG, Nichols NB (1942) Optimum setting for automatic controllers. *ASME Trans* 64(8):759–768

Publisher's Note Springer Nature remains neutral with regard to jurisdictional claims in published maps and institutional affiliations.

Springer Nature or its licensor (e.g. a society or other partner) holds exclusive rights to this article under a publishing agreement with the author(s) or other rightsholder(s); author self-archiving of the accepted manuscript version of this article is solely governed by the terms of such publishing agreement and applicable law.